Journal of Advanced Research in Numerical Heat Transfer

Journal homepage:
https://semarakilmu.com.my/journals/index.php/arnht/index
ISSN: 2735-0142

Nonlinear Mixed Convective Flow of Darcy-Forchheimer Maxwell Tri-Hybrid Nanofluid Past a Riga Plate

Abhilash Anand Kumar[1,*], Sreedhar Sobhanapuram[1], Mangali Veera Krishna[2]

[1] Department of Mathematics, GITAM (Deemed to be university), Visakhapatnam, Andhra Pradesh - 530045, India
[2] Department of Mathematics, Rayalaseema University, Kurnool, Andhra Pradesh - 518007, India

ARTICLE INFO

Article history:
Received 22 July 2024
Received in revised form 21 August 2024
Accepted 25 September 2024
Available online 30 October 2024

Keywords:
Maxwell Fluid; Ternary Hybrid Nanofluid; Nonlinear Mixed Convection; Darcy-Forchheimer Law

ABSTRACT

This contribution aims to explain the nonlinear thermal flow for Darcy-Forchheimer Maxwell tri-hybrid nanofluid flow over a Riga wedge in the context of boundary slip. Three types of nanomaterials, alumina, Copper and Titania have been mixed into the base fluid known as engine oil. Thermal properties with the effects of porous surface and nonlinear mixed convection have been established for the particular combination. Applying a set of appropriate variables, the couple of equations that evaluated the energy and flow equations was transferred to the non-dimensional form. For numerical computing, the MATLAB software's bvp4c function is used. This article looks at how distinct dimensionless parameters affect the velocity field, temperature distribution, drag force, and Nusselt number. It has been detected that flow rate decay with expansion in porosity parameter and nanoparticles volumetric fractions whereas it rises with wedge angle, Grashof numbers, Darcy-Forchheimer, nonlinear Grashof number and Maxwell fluid parameter. Thermal profiles increase with progress in the heat source, nanoparticles volumetric fractions, viscus dissipation and nonlinear thermal radiation. The percentage increase in skin friction factor is 18.3 and 15.0 when Mh and m take input in the ranges of $0.1 \leq Mh \leq 0.3$ and $0.1 \leq m \leq 0.3$.

1. Introduction

The widely held of the instigators exercised gelatinous (Newtonian) fluids to exemplify the flow mechanism. To the scope that microfluidic devices were utilized to explore the biofluids, however, this is inadequate. For the reason that of its exploits in industry, non-Newtonian liquids have fascinated a enormous compact of concentration. There is plentiful modelling for non-Newtonian fluids since of the involvedness of fluids. The Maxwell fluids modelling is the largely uncomplicated linear modelling to depicts the non-Newtonian fluids features for which this is realistic to be expecting that accurated and/or systematic resolutions would ultimately be revealed. The nanofluids were innovative substance that have never-ending applications in engineering, biological, medicinal as well as other fields. The magnitude of slip conditions in the macroscopic impacts of molecular proceduree s cannot be overstated.

* *Corresponding author.*
E-mail address: vanu_abhi@yahoo.co.in (Abhilash Anand Kumar)

https://doi.org/10.37934/arnht.25.1.5372

The stream difficulties are widely present in channels and tubes in a few physiological and engineering approaches. These streams expand during activities like being swallowed pee transportation from the kidney to the gallbladder, chyme evaluation in the intestines, ovum development in the female fallopian tubes, spermatozoa motions in the peristaltic mediums of the male conceptive system, vasomotion of narrow veins, heart, transport of mordant liquids, and other physiological processes. These activities are all supported by peristalsis. Due to its ability to conduct heat, the concept of nanofluid in peristalsis has recently attracted the interest of many researchers. Researchers have tried several methods throughout the years to increasing the thermal efficiency of liquids, such as transforming the shape of the material or adding chemicals. In order to achieve this, Maxwell added solid metallic particles into the base fluids in 1881. In order to increase the resistance of base liquids, microsized particles are utilized to create suspensions. However, the existence of these particles significantly increased the flow resistance. These particles are hefty and have a tendency to become residual. The human body uses peristalsis to move urine through the urethras and transport bile from the gall bladder.

Non-Newtonian fluids are complicated fluids that cannot be represented by a solitary relationship. Many applications, such as ketchup, sugar solutions, apple sauce, starch suspensions, soaps, lubricants, and margarine, can be described as displaying non-Newtonian fluid characteristics. A rate type subclass called the Maxwell fluid is a non-Newtonian representation that displays stress relaxation behaviours. Scientists are eager to learn more about its unique characteristics. Because of the broad array of uses that eventuate in engineering, industry and natural processes such as cooling of electronic equipment, human transpiration, some biological fluids, DNA suspension, escalation of chemicals in plants or medicine, aerodynamic extrusion, and many others, it has gained remarkable significance and expanded motivations or consciousness between many scientists to do work in the area over the last couple of years. Some remarkable contributions towards Maxwell nanofluid are done by well-known researchers in recent research work. Bilal *et al.,* [1] examined the radiation heat flux of MHD Maxwell fluid over an upper-connected surface. Jamshed *et al.,* [2] studied the various aspects of MHD Maxwell nanofluids. The chemical reactions on Maxwell flow via permeable surface under the effect of radiations and multiple slips have been inspected by Ali *et al.,* [3]. Abdal *et al.,* [4,5] reported PHF and PST properties on MHD Maxwell fluid containing living organisms. Bilal *et al.,* [6] analyzed the numerical simulation of time-dependent Maxwell flow of nanofluids inspired by melting heat, magnetic fields, Fourier and Fick laws. The liquid temperature drops when compared to melting heat and unsteadiness parameters, according to this study. Tlili *et al.,* [7] evaluated the flow of a 3D solutal and thermal stratification on Maxwell nanofluid with a chemical process. Yahya *et al.,* [8] studied the heat transfer analysis and viscous dissipation accomplish on Maxwell hybrid (SiO_2+TiO_2/Kerosene oil) nanofluid over a Riga wedge. Several investigators have disclosed various characteristics of the Maxwell liquid [9-13].

Darcy's law, which describes how liquid flows via a porous channel, is whence Darcy-Forchheimer (DF) gets its name. Based on the findings of an investigation of flowing water over the sand layer, this law was established. Movement is brought on by fluctuations in Reynolds numbers in the porous medium, where inertial forces are prominent. The significant usage of the DF law in petroleum technologies, grain storage, groundwater, and oil asset contexts make it essential for the study of fluid mechanics. In 1856, Darcy [14] was the first researcher to claim that liquid may pass through a porous surface. Unfortunately, this idea could not be as well-known due to its limits of the slower pace and lower porosity. Forchheimer [15] changed the equation of motion by substituting the quadratic velocity requirement with the Darcian velocity to show the obvious deficiency. The high Reynolds number led Muskat [16] to coin the phrase "Forchheimer word" to describe it. To implement the DF model to permeable media outside of the linearly enlarged zone, Pal and Mondal

[17] assumed that as the electric field value increases, the concentration distribution diminishes. The flow of the MHD nanofluid via the DF media platform as a result of the second-order boundary condition is computed by Ganesh *et al.,* [18]. DF law, homogeneous/heterogeneous reactions and carbon nanotubes were used by Alshomrani *et al.,* [19]. The DF effect was assessed over a curving surface by Saif *et al.,* [20]. Seth *et al.,* [21] computed the flow of CNTs in a moving frame across a porous DF environment. Several researchers have worked on DF law in the references [22-34].

The insert of nano-size particles into a base fluid has revolutionised the field of fluid dynamics. Single-type nanoparticles are amalgamated with the base fluid to create a nanofluid. Water, oils, ethylene glycol and synthetic fluids are commonly used to disseminate nanoparticles. These fluids are not capable for improve heat transfer as compared to nanofluids. Metallic nanoparticles such as silver, gold, titanium, iron oxide, aluminium and others are widely utilized in the base fluid. These liquids are used in thermal transfer systems as coolants like pharmaceutical processes, heat exchangers, engines, power plants, radiators, and electrical devices, among other things. Choi [35] first used nanoparticle dispersion in a host fluid to improve its thermal characteristics. Shafiq et al., [36], Sadiq *et al.,* [37], and Siddique *et al.,* [38-41] have all made significant contributions to improving the thermal properties of base fluids. A base fluid with a better thermal conductivity that contains two different types of nanoparticles in a mixture is referred to as a hybrid nanofluid. Hybrid nanofluids simultaneously increase the chemical and physical properties of constituents. In comparison to ordinary fluids and nanofluids, hybrid nanofluids have a significant impact on optimizing heat transfer since they have higher thermal efficiency and can be moulded to meet specific needs. The specific Stoke's second assumption approach was put to the test by Roy *et al.,* [42] utilising hybrid nanofluid. Shehzad *et al.,* [43] evaluated heat conduction through a permeable zone in a radiative hybrid nanofluid. Acharya *et al.,* [44] searched the role of radiation on hybrid (Fe_3O_4/graphene) nanofluid flow via a folded surface. The literature has a variety of research on hybrid nanofluids due to their effectiveness and applicability [45–50]. Ternary hybrid nanofluid (THN) is a novel type of fluid that leads regular fluids, nanofluid, hybrid nanofluid, acetone, and gasoline at energy exchanges. THNs are used in heat pumps, solar energy, heat exchangers, the auto industry, air purifiers, electrical chillers, broadcasters, ships, turbines, nuclear networks, and biotechnology. Adun *et al.,* [51] discussed the stability, heat transfer, environmental factors and synthesis of THN. Sundar *et al.,* [52] addressed irreversibility generation and heat transport over the surface based on THN. The rise of heat transmission for THN over a square channel was deliberated by Ahmed *et al.,* [53]. Their findings proved that THNs are better for thermophoresis and nano-cooling growth. Arif *et al.,* [54] considered the performance of heat transmission and flow for various shaped nanoparticles based on THNs. Gul and Saeed [55] addressed the enhancement of the thermal flow of the couple stress THN (TiO_2+$CoFe_2O_4$+MgO/H_2O) over a nonlinearly expanding sheet with DF law.

Jan *et al.,* [56] discussed the non-similar analysis of magnetized Sisko nanofluid flow subjected to heat generation/absorption and viscous dissipation. Jan *et al.,* [57] explored the heat transfer enhancement of forced convection magnetized cross model ternary hybrid nanofluid flow over a stretching cylinder. Farooq *et al.,* [58] discussed the non-similar mixed convection analysis of ternary hybrid nanofluid flow near stagnation point over vertical Riga plate. Cui *et al.,* [59] explored the non-similar aspects of heat generation in bioconvection from flat surface subjected to chemically reactive stagnation point flow of Oldroyd-B fluid. Farooq *et al.,* [60] explored the influence of slip velocity on the flow of viscous fluid through a porous medium in a permeable tube with a variable bulk flow rate.

Kumar *et al.,* [61] explored the simultaneous effects of nonlinear thermal radiation and Joule heating on the flow of Williamson nanofluid with entropy generation. Kumar *et al.,* [62] discussed the shape effect of nanoparticles and entropy generation analysis for MHD flow of hybrid nanomaterial under the influence of Hall current. Sethy *et al.,* [63] investigated the synergistic impacts of radiative flow of Maxwell fluid past a rotating disk with reactive conditions. Tripathi *et al.,* [64] discussed the minimization of entropy production in the transient thermocapillary flow of hybrid nanoliquid film over a disk. Kumar *et al.,* [65] explored the unsteady mixed convective flow of hybrid nanofluid past a rotating sphere with heat generation/absorption.

Keeping the abovementioned facts, the nonlinear thermal flow for Darcy-Forchheimer Maxwell tri-hybrid nanofluid flow over a Riga wedge in the context of boundary slip has not been studied yet. Therefore, in this paper, the nonlinear thermal flow for Darcy-Forchheimer Maxwell tri-hybrid nanofluid flow over a Riga wedge in the context of boundary slip has been explored. It is explored the three types of nanomaterials, Alumina, copper and Titania have been mixed into the base fluid known as engine oil. Thermal properties with the effects of porous surface and nonlinear mixed convection have been established for the particular combination tri-hybrid nanofluid. Applying a set of appropriate variables, the couple of equations that evaluated the energy and flow equations was transferred to the non-dimensional form. For numerical computing, the MATLAB software's bvp4c function is used.

2. Formulation and Solution of the problem

Assume that steady, the nonlinear thermal flow for Darcy-Forchheimer Maxwell tri-hybrid nanofluid flow over a Riga wedge in the context of boundary slip. The THN (Al_2O_3+Cu+TiO_2/EO) flows on stream (*x*-axis) coordinates which operate along the vertical Riga wedge surface, while transverse (*y*-axis) coordinates are normal to the surface as shown in Figure 1. Convective heat, porosity kp, and the slip effect are also taken into account. $u_{sv} = U_{sv}x^m$ shows free stream velocity while U_{sv} is constant. Here, $u_v = U_v x^m$ signifies the wedge's extended velocity whereas $U_v > 0$ recognizing the expanding wedge. Further, $m = \psi/(2-\psi)$, where the wedge angle is ψ, $m\ (0 < m < 1)$ is the Hartree pressure gradient, and $\varpi = \psi\pi$ determines the wedge's fixed total angle. Also, $T_f > T_\infty$, where T_∞ and T_f is ambient and the surface temperature, respectively.

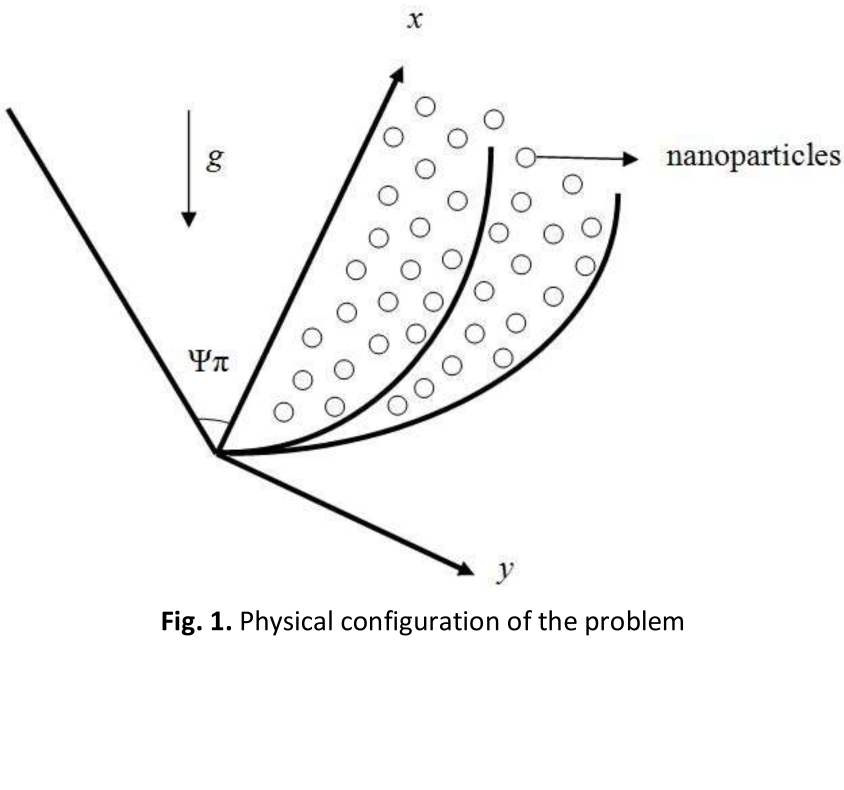

Fig. 1. Physical configuration of the problem

The essential assumption of [1,6,8] provides the fundamental equations for THN flow

$$\frac{\partial u}{\partial x}+\frac{\partial v}{\partial y}=0, \tag{1}$$

$$u\frac{\partial u}{\partial x}+v\frac{\partial u}{\partial y}=\frac{\mu_{trhnf}}{\rho_{trhnf}}\frac{\partial^2 u}{\partial y^2}+u_{sv}\frac{du_{sv}}{dx}-\frac{\mu_{trhnf}}{\rho_{trhnf}k^*}u-\frac{F}{\rho_{trhnf}}u^2+\frac{\lambda_1}{\rho_{trhnf}}\left(u^2\frac{\partial^2 u}{\partial x^2}+v^2\frac{\partial^2 u}{\partial y^2}+2uv\frac{\partial^2 u}{\partial xy}\right)$$
$$+\frac{\rho_f J_0 M_0 \pi}{8\rho_{trhnf}}e^{\left(-\pi/_d\right)y}+\frac{g}{\rho_{trhnf}}\left[\alpha_1\left(T-T_\infty\right)+\alpha_2\left(T-T_\infty\right)^2\right]Cos\left(\pi\psi/_2\right), \tag{2}$$

$$u\frac{\partial T}{\partial x}+v\frac{\partial T}{\partial y}=\frac{k_{trhnf}}{\left(\rho c_p\right)_{trhnf}}\frac{\partial^2 T}{\partial y^2}+\frac{\mu_{trhnf}}{\left(\rho c_p\right)_{trhnf}}\left(\frac{\partial u}{\partial y}\right)^2+\frac{Q_0}{\left(\rho c_p\right)_{trhnf}}\left(T-T_\infty\right)-\frac{1}{\left(\rho c_p\right)_{trhnf}}\frac{\partial q_r}{\partial y}, \tag{3}$$

The boundary conditions are:

$$\left.\begin{aligned}&v(x,0)=0,\ u_w+\mu_{trhnf}\frac{\partial u}{\partial y}=u(x,0),\ -k_{trhnf}\frac{\partial T}{\partial y}=h_f\left(T-T_w\right),\ \text{at } y\to 0,\\&u\to u_e,\ T\to T_\infty,\ \text{at } y\to\infty,\end{aligned}\right\} \tag{4}$$

where, the permanently magnetized magnate is named M_0. The nanofluids, hybrid and ternary nanofluids are converted to a Maxwell fluid by putting $\phi_1=\phi_2=\phi_3=0$. Here the heat capacity $\left(\rho C\right)p_{trhnf}$, dynamic viscosity μ_{trhnf}, electrical conductivity σ_{trhnf}, the liquid density ρ_{trhnf}, specific heat Cp_{trhnf}, and thermal conductivity of ternary hybrid nanofluid k_{trhnf}. For Al_2O_3, Cu and TiO_2 nanoparticles, the subscripts f, nf, hnf, $trhnf$, s_1, s_2 and s_3 signify the fluid, nanofluid, HN, THN and solid components, accordingly. According to the Roseland approximation for radiation in Eq. (3), q_r is the radiative heat flow is defined as follows:

$$q_r=-\frac{4\delta^{**}}{3k^{**}}\frac{\partial T^4}{\partial y}=-\frac{16\delta^{**}T^3}{3k^{**}}\frac{\partial T}{\partial y}$$

$$\frac{\partial q_r}{\partial y}=-\frac{16\delta^{**}}{3k^{**}}\left(T^3\frac{\partial^2 T}{\partial y^2}+3T^2\left(\frac{\partial T}{\partial y}\right)^2\right), \tag{5}$$

where k^{**} and δ^{**} are the delegate of mean absorption coefficient and Stefan-Boltzman constant respectively.

After placement of Eq. (5) into Eq. (3), the final equation is written as follows:

$$u\frac{\partial T}{\partial x}+v\frac{\partial T}{\partial y}=\frac{k_{trhnf}}{\left(\rho c_p\right)_{trhnf}}\frac{\partial^2 T}{\partial y^2}+\frac{\mu_{trhnf}}{\left(\rho c_p\right)_{trhnf}}\left(\frac{\partial u}{\partial y}\right)^2+\frac{16\delta^{**}}{3\left(\rho c_p\right)_{trhnf}k^{**}}\left(T^3\frac{\partial^2 T}{\partial y^2}+3T^2\left(\frac{\partial T}{\partial y}\right)^2\right)$$
$$+\frac{Q_0}{\left(\rho c_p\right)_{trhnf}}\left(T-T_\infty\right), \tag{6}$$

For the Eqs. (1), (2), (6) and BCs (4) the subsequent similarity transformations are publicized in Eq. (7) [8]. Here the stream function (ω) can be indicated as $u=\partial\omega/\partial y$, and $v=-\partial\omega/\partial x$.

$$\omega=\sqrt{U_{sv}\nu_f}\,x^{(m+1)/2}f(\eta),\ \ \eta=\sqrt{\frac{U_{sv}}{\nu_f}}x^{(m-1)/2}y,\ \ \theta(\eta)=\frac{T-T_\infty}{T_f-T_\infty},\ u=U_{sv}x^m f'(\eta),$$
$$v=-\sqrt{U_{sv}\nu_f}\,x^{(m-1)/2}\left(\frac{m+1}{2}\right)\left(\frac{m-1}{m+1}\eta f'(\eta)+f(\eta)\right), \tag{7}$$

Eqs. (2)–(4) transformed into a collection of ODEs by retaining Eq. (7):

$$\frac{\mu_r}{\rho_r}\left(\frac{m+1}{2}\right)f'''-(f')^2+\left(\frac{m+1}{2}\right)ff''+m+\frac{Mh\exp(-ah\eta)}{\rho_r}-\frac{\mu_r}{\rho_r}kpf'-\frac{F_r}{\rho_r}(f')^2$$
$$-\frac{\lambda}{\rho_r}\left\{m(m-1)(f')^3+\left(\frac{m-1}{2}\right)^2\eta(f')^2f''+\left(\frac{m+1}{2}\right)^2f^2f'''-\left(\frac{m-1}{2}\right)^2\eta^2f'''(f')+\right.$$
$$\left.+m\left(\frac{m+1}{2}\right)fff''+\left(\frac{m^2-1}{4}\right)fff''\right\}+\frac{\beta_1}{\rho_r}\theta(1+\beta_2\theta)=0, \tag{8}$$

$$\frac{k_r}{(\rho Cp)_r}\theta''+\frac{\mathrm{Nr}}{(\rho Cp)_r}\left(1+\theta(\theta_r-1)\right)^3\theta''+\frac{3\,\mathrm{Nr}}{(\rho Cp)_r}(\theta')^2(\theta_r-1)\left(1+\theta(\theta_r-1)\right)^2$$
$$+\frac{2\Pr\theta H}{(\rho Cp)_r(m+1)}+\Pr f\theta'+\frac{\Pr Ec\mu_r}{(\rho Cp)_r}(f'')^2=0, \tag{9}$$

with BCs are

$$\left.\begin{aligned}&f(\eta)=0,\ 1+\gamma\mu_r f''(\eta)=f'(\eta),\ \ k_r\theta'(\eta)=-\left(1-\theta(\eta)\right)Bi,\ \text{ at }\ \eta\to 0,\\&f'(\eta)=1,\ f''(\eta)=0,\ \theta(\eta)=0,\ \text{at }\ \eta\to\infty,\end{aligned}\right\} \tag{10}$$

where *Fr* is Darcy parameter, modified Hartmann number $Mh=\frac{\pi j_0 M_0}{4u_{sv}^2}$, Maxwell fluid parameter $\lambda=\frac{2\lambda_1 b}{\mu_f}$, temperature difference $\theta_r=\frac{T_f}{T_\infty}$, non-dimensional parameter $ah=\frac{\pi}{d}\sqrt{\frac{2\nu_f}{m+1}}$, slip parameter $\gamma=\sqrt{\frac{U_{sv}}{\nu_f}}R\mu_f$, Prandtl number $\Pr=\frac{\alpha_f}{\nu_f}$, local Grashof number

$Grx = \frac{g\alpha_1 x^3 \left(T_w - T_\infty\right) Cos\left(\pi\psi/2\right)}{\nu_f^2}$, nonlinear convection parameter $\beta_2 = \frac{\alpha_2\left(T_w - T_\infty\right)}{\alpha_1}$, mixed convection parameter $\beta_1 = \frac{Grx}{\mathrm{Re}_x^2}$, local Reynolds number $\mathrm{Re}_x^2 = \frac{u_v x}{\nu_f}$, heat source parameter $H = \frac{Q_0}{\left(\rho Cp\right)_f}$, thermal radiation $Nr = \frac{-16\delta^{**} T_\infty^3 a}{3k^{**} k_f}$, and Biot number $Bi = \frac{h_f}{k_f}\sqrt{\frac{2x\nu_f}{U_{sv}\left(m+1\right)}}$.

The thermophysical properties of the THNs are [41-42,45]:

$$\mu_r = \frac{\mu_{trhnf}}{\mu_f} = \left(1-\phi_1\right)^{-2.5}\left(1-\phi_2\right)^{-2.5}\left(1-\phi_3\right)^{-2.5},$$

$$\rho_r = \frac{\rho_{trhnf}}{\rho_f} = \left(1-\phi_1\right)\left(\left[\left(1-\phi_2\right)\left\{\left(1-\phi_3\right) + \frac{\rho_{s_3}\phi_3}{\rho_f}\right\} + \frac{\rho_{s_2}\phi_2}{\rho_f}\right]\right) + \frac{\rho_{s_1}\phi_1}{\rho_f}, \quad \alpha_{trhnf} = \frac{k_{trhnf}}{\left(\rho c_P\right)_{trhnf}}$$

$$\left(\rho C_\rho\right)_r = \frac{\left(\rho C_\rho\right)_{trhnf}}{\left(\rho C_\rho\right)_f} = \left(1-\phi_1\right)\left(\left[\left(1-\phi_2\right)\left\{\left(1-\phi_3\right) + \frac{\left(\rho C_\rho\right)_{s_3}\phi_3}{\left(\rho C_\rho\right)_f}\right\} + \frac{\phi_2\left(\rho C_\rho\right)_{s_2}}{\left(\rho C_\rho\right)_f}\right]\right) + \frac{\phi_1\left(\rho C_\rho\right)_{s_1}}{\left(\rho C_\rho\right)_f},$$

$$k_r = \frac{k_{trhnf}}{k_{hnf}} = \frac{2k_{hnf} - 2\phi_1\left(k_{s_1} - k_{hnf}\right) + k_{s_1}}{2k_{hnf} + \phi_1\left(k_{s_1} - k_{hnf}\right) + k_{s_1}}, \frac{k_{hnf}}{k_{nf}} = \frac{2k_{nf} - 2\phi_2\left(k_{s_2} - k_{nf}\right) + k_{s_2}}{2k_{nf} + \phi_2\left(k_{s_2} - k_{nf}\right) + k_{s_2}},$$

$$\frac{k_{nf}}{k_f} = \frac{2k_f - 2\phi_3\left(k_{s_3} - k_f\right) + k_{s_3}}{2k_f + \phi_3\left(k_{s_3} - k_f\right) + k_{s_3}}. \tag{11}$$

Eq. (11) reveals the physical characteristics of engine oil, Al_2O_3, Cu and TiO_2 nanoparticles. Table 1 provides an overview of the thermal characteristics of nanofluids, hybrid nanofluids, and ternary nanofluids.

Table 1
The Al_2O_3 and Cu thermo-physical properties along with TiO_2 and EO [20-25]

Physical properties	$\rho\left(kg/m^3\right)$	$C_p\left(J/kgK\right)$	$k\left(\mathrm{W}/mK\right)$
EO	884	1910	0.144
Al_2O_3	3970	765	40
Cu	8933	385	401
TiO_2	4230	692	8.4

The skin friction $\left(Cf_x\right)$ and Nusslt number $\left(Nu_x\right)$ are defined by [5,6,8]

$$Cf_x = \frac{1}{\rho_f u_v^2}\left[\mu_{trhnf}\left(1+\lambda_1\right)\frac{\partial u}{\partial y}\right]_{y=0} \tag{12}$$

$$Nu_x = -\frac{x}{k_f\left(T_w - T_\infty\right)}\left[k_{trhnf} + \frac{16\sigma^* T_\infty^3}{3k^*}\right]\left(\frac{\partial T}{\partial y}\right)_{y=0} \tag{13}$$

Then incorporate Eq. (7) to Eqs. (12) and (13), resulting in the relationship shown below:

$$\sqrt{\mathrm{Re}_x} Cf_x = \mu_r \left(1+\lambda\right) f''\left(0\right), \tag{14}$$

$$\left(\mathrm{Re}_x\right)^{-0.5} Nu_x = -\left(k_r + Nr\left(1+\theta\left(0\right)\left(\theta_w - 1\right)\right)^3\right)\theta'\left(0\right). \tag{15}$$

The Maxwell fluid's governing flow equations are incredibly nonlinear, and due to their tremendous complexity, it is impossible to find exact solutions. As a result, a numerical approach can be used to find the solution. Through the transformation of the current controlling problems into related first-order equations,

$$f\left(\eta\right) = G_1,\ f'\left(\eta\right) = G_2,\ f''\left(\eta\right) = G_3,\ f'''\left(\eta\right) = G_4,\ f''''\left(\eta\right) = G_4',\ \theta\left(\eta\right) = G_5,\ \theta'\left(\eta\right) = G_6, \tag{16}$$

$$G_4' = \frac{2\rho_r}{\alpha\left(m+1\right)G_1}\left[\begin{array}{l}\dfrac{\mu_r}{\rho_r}G_4 + \left(\dfrac{2m}{m+1}\right)\left(1-\left(G_2\right)^2\right) + \dfrac{\alpha}{\rho_r}\left(\begin{array}{l}\left(3m-1\right)G_2G_3 + \left(\dfrac{3m-1}{2}\right){G_3}^2 \\ +\left(m-1\right)\eta G_3G_4\end{array}\right) \\ +Mh\exp\left(-ah\eta\right) + G_1G_3\end{array}\right], \tag{17}$$

$$G_6' == \frac{-\left(\rho Cp\right)_r}{k_r + \left(1+G_5\left(\theta_r - 1\right)\right)^3}\left[\frac{3\,\mathrm{Nr}}{\left(\rho Cp\right)_r}\left(G_6\right)^2\left(\theta_r - 1\right)\left(1+G_5\left(\theta_r - 1\right)\right)^2 + \frac{\mathrm{Pr}\,G_5 H}{\left(\rho Cp\right)_r} + \mathrm{Pr}\,G_1G_6\right], \tag{18}$$

with boundary conditions are

$$\begin{array}{l} G_1 = 0,\ G_2 = 1 + \gamma\mu_r G_3\left(\eta\right),\ k_r G_6\left(\eta\right) = -Bi\left(1 - G_1\left(\eta\right)\right), \text{ at } \eta \to 0, \\ G_2\left(\eta\right) = 1,\ G_3\left(\eta\right) = 0,\ G_5\left(\eta\right) = 0, \text{ at } \eta \to \infty. \end{array} \tag{19}$$

By using the bvp4c technique in MATLAB, the aforementioned set of ODEs (16), (17) and (18) with BCs (19) was numerically solved with 10^{-6} residual-error.

3. Results and discussion

The goal of this research is to use Maxwell THNs flowing over a Riga wedge for efficient applications of cooling and heating in thermal engineering. The THN comprises solid nanoparticles such as Al_2O_3, Cu and TiO_2 with EO as a base liquid. The solid particles dissolve in the base liquid, resulting in the formation of the THN. Thermal properties were found using the combination Al_2O_3+Cu+TiO_2/EO under the appearance of nonlinear thermal radiations and convection associated with the porous surface.

It takes into consideration the standard set of fluid flow variables such as $Nr = 4.0,\ Mh = 0.5,$ $kp = 0.2,\ \mathrm{Fr} = 0.3,\ Ec = 0.6,\ \beta_1 = 0.2,\ \beta_2 = 0.5,\ \ \mathrm{Pr} = 50,\ H = 0.1,\ m = 0.3,\ ah = 0.2,\ \theta_r = 1.2,\ \alpha = 0.3$, $Bi = 0.8,\ \lambda = 0.3,\ \mathrm{Re} = 0.5$ and $\phi_1 = \phi_2 = \ \phi_3 = 0.01.$ The influence of the constraints is portrayed in Figures 2-19.

In Table 2, we compare the heat transmission rate with existing data from Yahya et al., [8] for numerous values of *Pr*. An exceptional match was witnessed, which validates the numerical technique and the resultant outcomes.

Table 2
Comparison of $-\theta'(0)$ for several values of *Pr* when $Kp = H = Mh = Nr = \lambda = \beta_1 = Nr = Ec = 0$

Pr	Yahya *et al.,* [8]	Present results
0.71	0.911411452788	0.911414788512
6.13	1.759547885455	1.759655896521
7.00	1.895474485545	1.895212258996
20.0	3.354096620114	3.353999856322

The inspiration of *Mh* and the *ah* on $f'(\eta)$ is appreciated in Figures 2 and 3. The argument is that for both fluids, velocity improves as *Mh* rises and falls as *ah* grows. The magnetism between the wedge's boundary is elevated by the complex principles of the *Mh*. Due to increased magnetism between the wedge boundary, the Riga wedge is more compact than the ordinary wedge. Also, *Mh* is associated with the Riga layout, which reduces the friction in the stream and hence accelerates it.

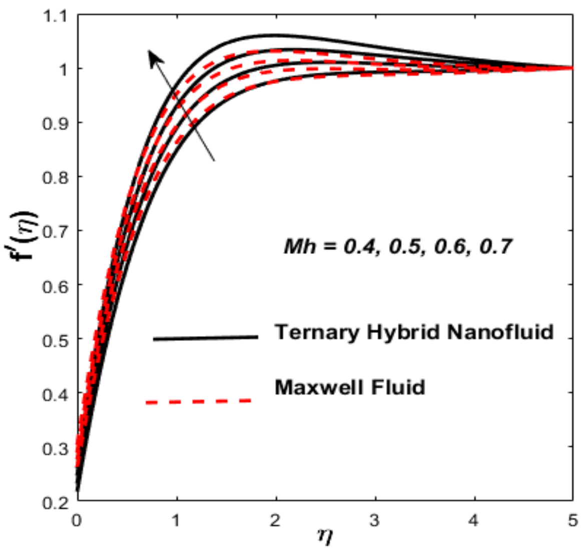

Fig. 2. Velocity profiles against Mh

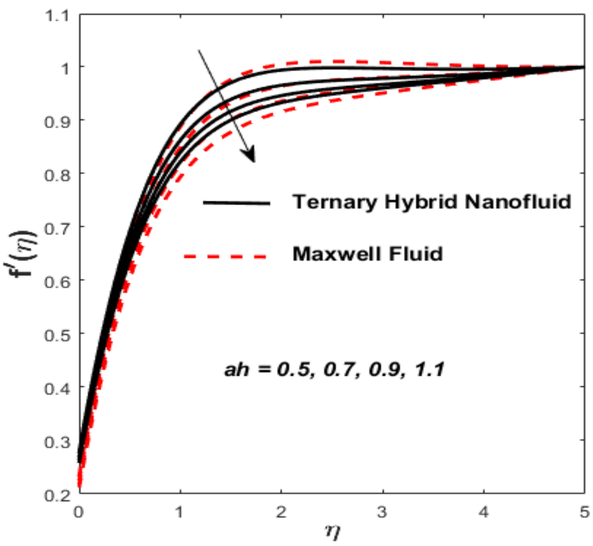

Fig. 3. Velocity profiles against ah

The outcomes of *m* on $f'(\eta)$ and thermal $\theta(\eta)$ profiles are exposed in Figures 4 and 5. Against *m*, the flow rate increase while the temperature drop. This inclination is caused by the fact that a higher wedge angle boosts fluid velocity, which forces the boundary layer's (BL) thickness to drop and the temperature to elevate.

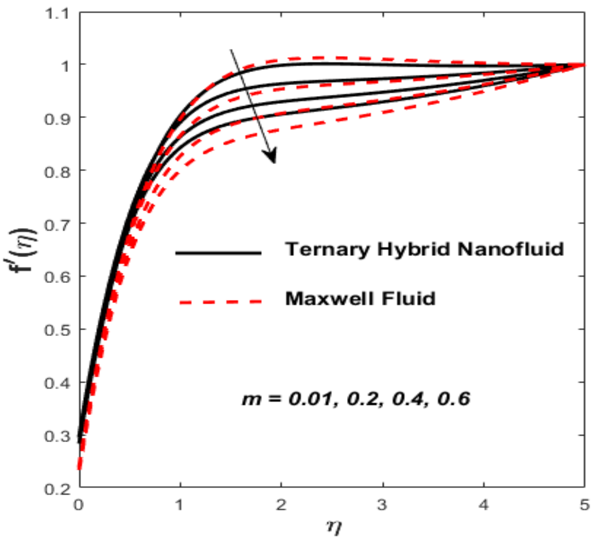

Fig. 4. Velocity profiles against m

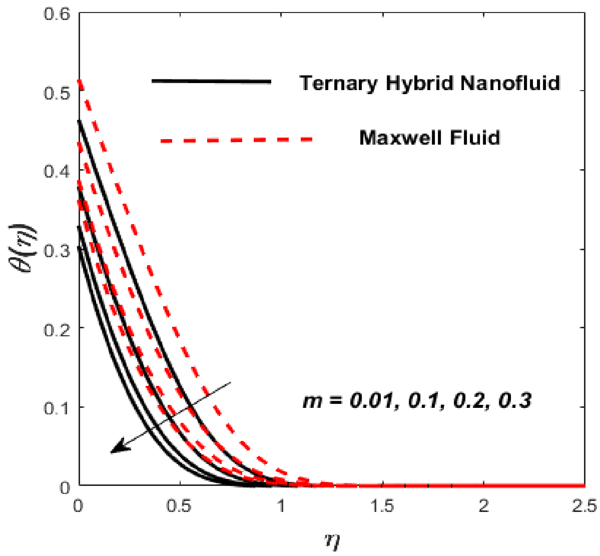

Fig. 5. Temperature profiles against m

The larger value of λ causes the fluid motion to grow and declines the heat transfer as publicized in Figures 6 and 7. As λ climbs, the resistance forces between the fluid particles and the surface of the wedge fall, resulting in insufficient resistance to fluid motion which rises in the flow rate and declines the heat transfer rate. Additionally, it is established that for the Maxwell fluid, the BL thickness grows. With higher λ, it is known that the hydrodynamic BL thickness rises.

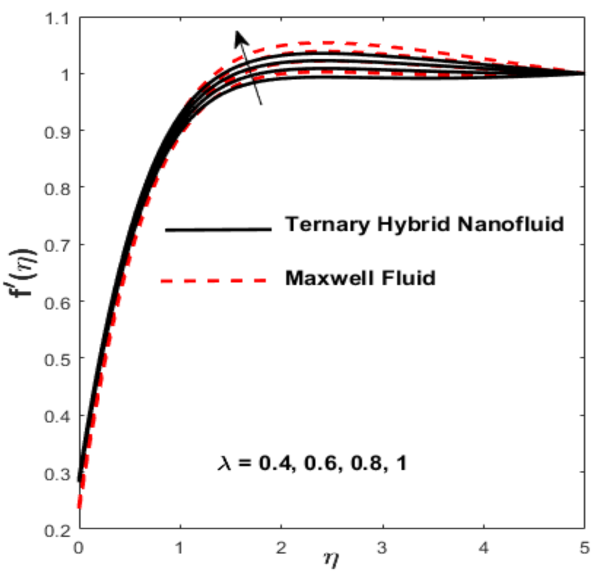

Fig. 6. Temperature profiles against λ

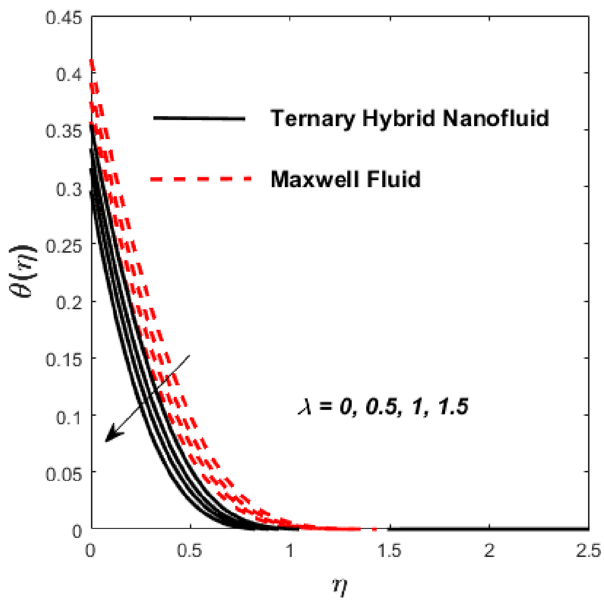

Fig. 7. Temperature profiles against λ

Figures 8 and 9 depicts the behaviour of $f'(\eta)$ in reaction to deviations in β_1 and β_2. The correlation between buoyancy and frictional forces is referred as the Grashof number; therefore, raising the values of β_1 and β_2 reduces the viscosity behaviour of nanoparticles, resulting in a slowdown in resistive forces to fluid motion.

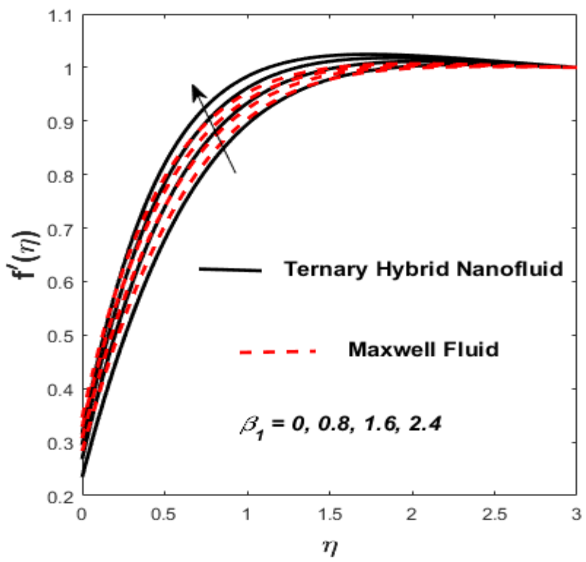

Fig. 8. Velocity profiles against β_1

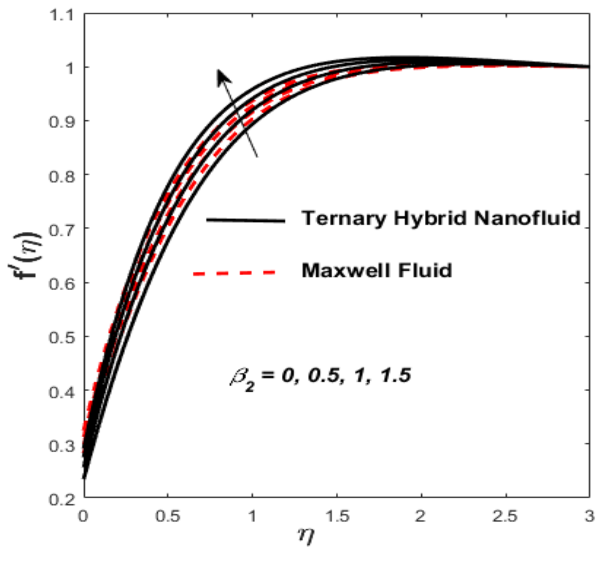

Fig. 9. Velocity profiles against β_2

The fluid's velocity increases in this physical phenomenon, as demonstrated in Figures 10 and 11 depicts how increasing levels of *kp* and *Fr* slow down fluid velocity. When *kp* and *Fr* climbed, the capacity of pore space enhanced, causing additional resistance to liquid motion and reducing the flow rate of the fluid.

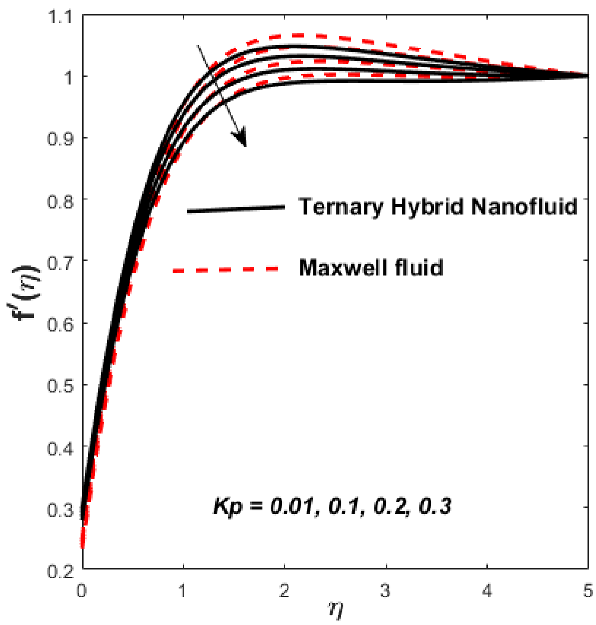

Fig. 10. Velocity profiles against kp

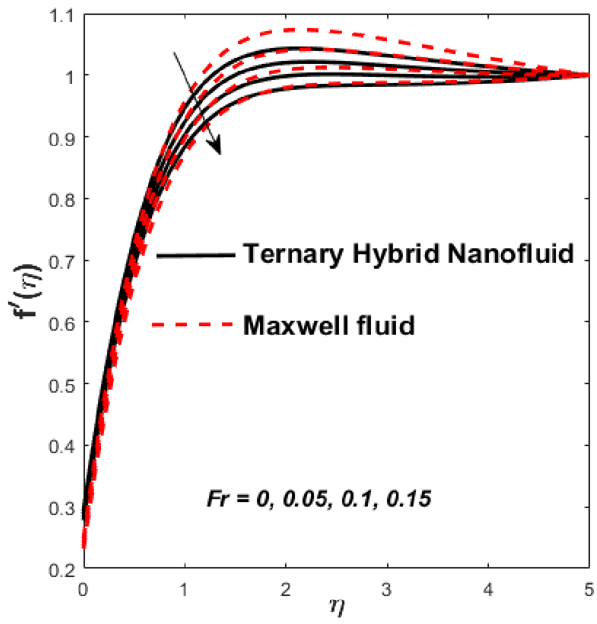

Fig. 11. Velocity profiles against Fr

The γ and Bi imprinted in Figures 12 and 13 represent the $f'(\eta)$ and $\theta(\eta)$. The γ and Bi lead the flow rate and thermal to raise, as has been displayed. It is believed that the γ will speed up the fluid motion and generate more disturbance. Logically, when the velocity slip improves, the fluid velocity grows, causing a rise in the forces needed to drive the expanding wedge and a transfer of energy to the liquid. However, it is reported that THN has the maximum velocity when compared to Maxwell fluid due to their improvement in thermophysical properties. So the Bi is used to calculate heat transmission rate, we can conclude that Bi has a direct relationship with thermal efficiency. Physically, elevating the values of the Bi improves the thermal proficiency of the fluid, causing an upsurge in the heat transmission rate.

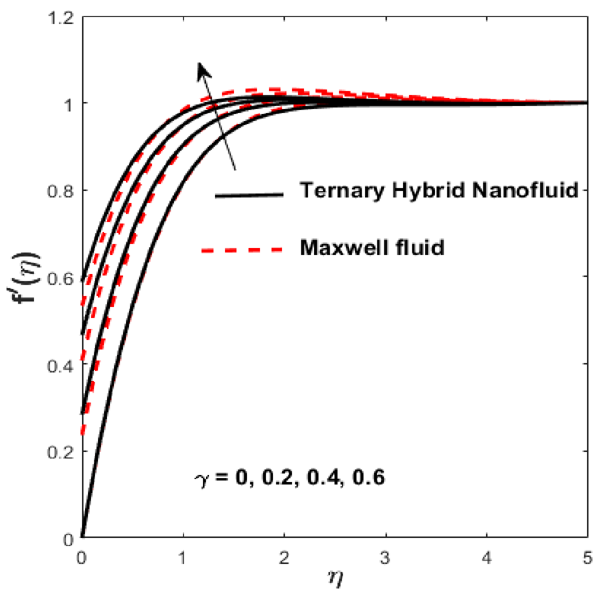

Fig. 12. Velocity profiles against γ

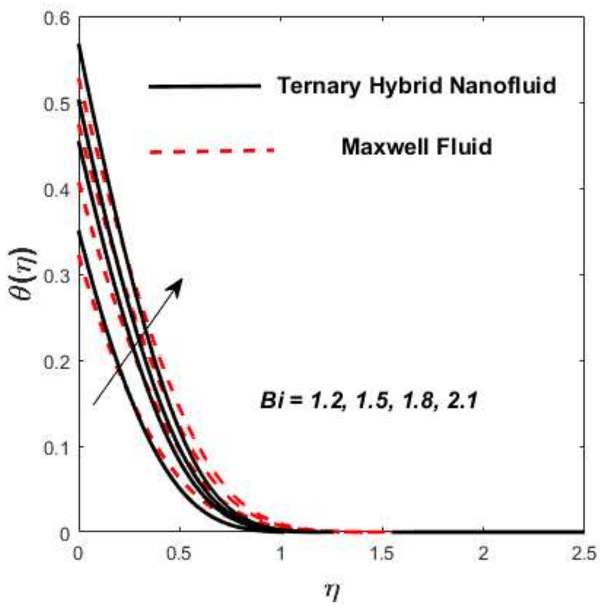

Fig. 13. Temperature profiles against Bi

The impression of *Nr* and θ_r on the $\theta(\eta)$ is demonstrated in Figures 14 and 15. It can be seen that the fluid temperature boost when θ_r and *Nr* are grown. A higher θ_r physically denotes a substantial thermal difference between the the surroundings and wedge wall. The thermal BL thickness boosts as a result of temperature variation. Tiny particles become more mobile due to the radiative component, which forces unrelated moving particles have a collision and convert frictional energy into thermal energy.

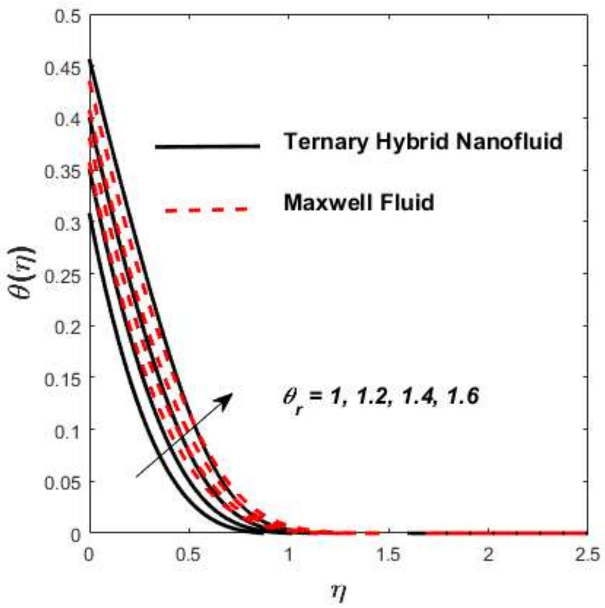

Fig. 14. Temperature profiles against θ_r

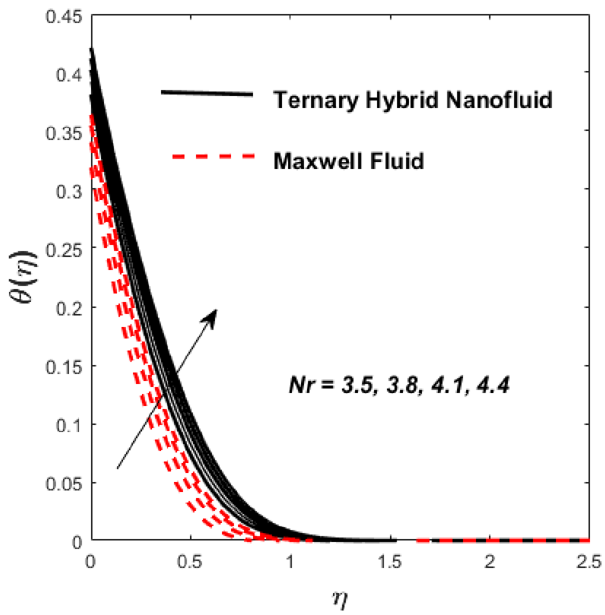

Fig. 15. Temperature profiles against Nr

The realize of *Ec* and *H* on $\theta(\eta)$ is highlighted in Figures 16 and 17. It is identified that as the *Ec* and *H* climb, the heat transfer boosts. Also, as compared to a Maxwell fluid, a THN has a faster heat transmission rate. The temperature profile is also improved due to the existence of dissipation effects in the energy equation. The main reason for this behind is that higher *Ec* values convert mechanical energy into thermal energy. During the cooling or heating process, a sizable amount of heat energy is discharged from the wedge, strengthening the thermal field in the BL region close to the wedge. The temperature profile also decays to zero at closer proximity to the wedge.

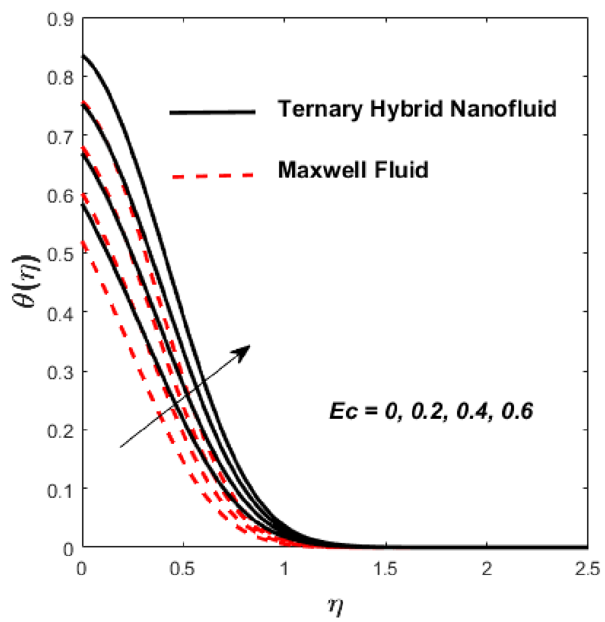

Fig. 16. Temperature profiles against Ec

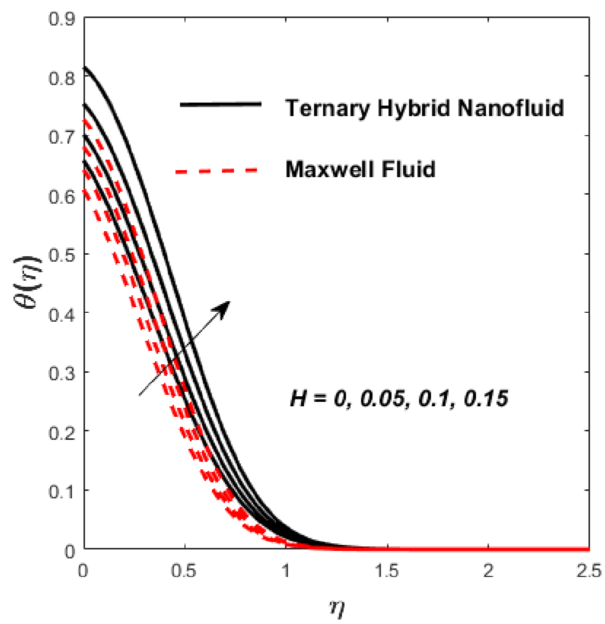

Fig. 17. Temperature profiles against H

Figures 18 and 19 illustrates how the $f'(\eta)$ and $\theta(\eta)$ of fluid and THNs are impacted by the ϕ_1, ϕ_2 and ϕ_3. It is reflected that with the enlargement of ϕ_1, ϕ_2 and ϕ_3, the fluid velocity declines while the fluid temperature is enhanced. Physically, the momentum and thermal BL become denser for the higher values of ϕ_1, ϕ_2 and ϕ_3 in the nanofluid, hybrid and THN, which generates extravagantly resistance in the fluid, and as a consequence, the velocity reduces, and due to the presence of these nanoparticles, the thermal conductivity of fluid goes up which ultimately rises the heat of the fluid. Furthermore, the THN exhibits the lowest velocity and the highest rate of heat transfer when compared to nanofluid and hybrid nanofluid. The base liquid releases more heat when more nanoparticles are inserted because there are more repulsion collisions between the fluids as a result. As either a consequence, THNs have a larger temperature dispersion over the wedge than liquids containing dual and single-phase nanoparticles.

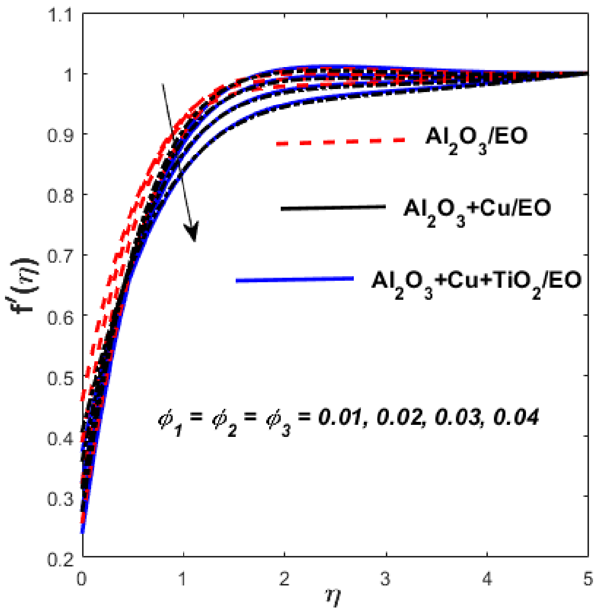

Fig. 18. Velocity profiles against ϕ_1, ϕ_2 and ϕ_3

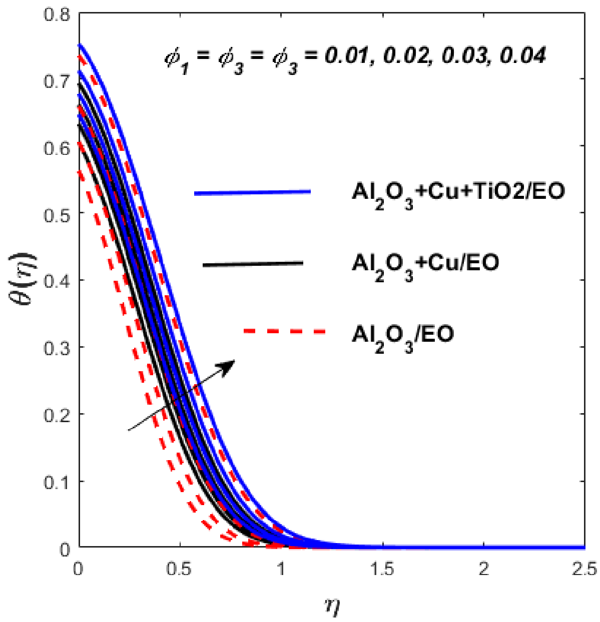

Fig. 19. Temperature profiles against ϕ_1, ϕ_2 and ϕ_3

Table 3 displayed the drag force and heat transfer rate for hybrid nanofluids (Al_2O_3+Cu/EO), THNs (Al_2O_3+Cu+TiO_2/EO) and Maxwell fluid. From Table 3, it is witnessed that skin friction is elevated via *Mh, m,* θ_r and *Ec* while the decline via *Kp* and *Fr*. Table 3 also demonstrates the numerical results for the surface heat transfer rate. In response to rising *kp*, *Fr* and θ_r values, the surface heat transfer rate for hybrid nanofluid and THN is notably amplified, and the Rising *Mh, m,* and *Ec* values produced the opposite effects, as was expected. A THN is thought to have a higher heat transfer rate than a hybrid nanofluid and Maxwell fluid.

Table 3
Numerical results of Maxell fluid, ternary nanofluid and hybrid nanofluid for Cf_x and Nu_x

						Ternary Hybrid Nanofluid		Hybrid Nanofluid		Maxwell Fluid	
Mh	*kp*	*Fr*	*m*	θ_r	*Ec*	Cf_x	Nu_x	Cf_x	Nu_x	Cf_x	Nu_x
0.1	0.2	0.3	0.3	1.2	0.6	1.20946340	0.22480898	1.18740717	0.21096564	1.12692867	0.17254997
0.2						1.32041704	0.17414448	1.29899300	0.15926282	1.24128462	0.11775656
0.3						1.43066608	0.11460706	1.409951451	0.098187698	1.35539755	0.05158148
	0					1.47662007	0.035330476	1.409671037	0.05246630	1.456676773	0.018791812
	0.1					1.35265815	0.130692771	1.291944403	0.14827692	1.335358627	0.078760446
	0.2					1.24518576	0.200603876	1.190668506	0.21851044	1.230237541	0.149444601
		0				1.38752745	0.090720066	1.337048423	0.11154737	1.373724821	0.031370683
		0.1				1.30879273	0.155053556	1.255184007	0.17395173	1.294145215	0.101316490
		0.2				1.24518576	0.20060387	1.190668506	0.21851044	1.230237541	0.14944460
			0.1			1.24826085	0.16804294	1.20842540	0.18707668	1.23580216	0.10909119
			0.2			1.35265815	0.13069277	1.291944403	0.14827692	1.33535862	0.078760446
			0.3			1.43066608	0.098187698	1.355397556	0.11460706	1.40995145	0.051581482
				1.2		1.110636890	0.27372544	1.05865331	0.291022040	1.09613152	0.22275048
				1.3		1.115430844	0.30764553	1.06340488	0.325157240	1.10096347	0.25499281
				1.4		1.12050629	0.37263249	1.06846402	0.39135205	1.10607857	0.31356048
					0.2	1.076875601	0.46751222	1.0214003	0.485055140	1.06182054	0.4201278
					0.3	1.085115482	0.41937058	1.0304512	0.436779575	1.07018676	0.3713418
					0.4	1.093486670	0.37104546	1.0396726	0.388368019	1.07869130	0.3222080

4. Conclusions

A comprehensive analysis of 2D Darcy's Forchheimer Maxwell THN flow towards a vertical Riga wedge with nonlinear mixed convection and thermal radiation is inspected. The following are some intriguing findings that were drawn from the current work:

i) It is demonstrated that ternary hybrid nanofluid is a better heat transfer than Maxwell fluid.
ii) The velocity profiles decline as the Darcy-Forchheimer and porosity parameters are enhanced.
iii) The heat transfer has increased as the Eckert number, heat source and nonlinear thermal radiation improve.
iv) Nonlinear convection and nanoparticle volume fractions slow down the velocity of the fluid whereas the opposite behaviour is noted for *Mh,* γ and *m*.
v) The skin friction upsurges with *Mh,* and *m* while the rising values of *kp* and *Fr* cause to diminish the magnitude of $-f''(0)$.
vi) Heat transfer is boosted in the case of a ternary nanofluid.
vii) When the input parameters *Mh* and *m* are used, the heat transfer rate of hybrid nanofluid is 18% and 15% while the heat transfer rates of THN are 7.03% and 8.71%, respectively.
viii) Ternary hybrid nanofluid show maximum heat transfer as compared to the hybrid nanofluid and nanofluid.
ix) With rising values of *kp, Fr* and θ_r progressive behaviour is shown for $-\theta'(0)$ but it is inversely proportional to *Ec, Mh,* and *m*.

References

[1] Bilal, M., M. Sagheer, and S. Hussain. "Three dimensional MHD upper-convected Maxwell nanofluid flow with nonlinear radiative heat flux." *Alexandria engineering journal* 57, no. 3 (2018): 1917-1925. https://doi.org/10.1016/j.aej.2017.03.039
[2] Jamshed, Wasim. "Numerical investigation of MHD impact on Maxwell nanofluid." *International Communications in Heat and Mass Transfer* 120 (2021): 104973. https://doi.org/10.1016/j.icheatmasstransfer.2020.104973
[3] Ali, Bagh, Yufeng Nie, Shahid Ali Khan, Muhammad Tariq Sadiq, and Momina Tariq. "Finite element simulation of multiple slip effects on MHD unsteady maxwell nanofluid flow over a permeable stretching sheet with radiation and thermo-diffusion in the presence of chemical reaction." *Processes* 7, no. 9 (2019): 628. https://doi.org/10.3390/pr7090628
[4] Abdal, Sohaib, Usama Habib, Imran Siddique, Ali Akgül, and Bagh Ali. "Attribution of multi-slips and bioconvection for micropolar nanofluids transpiration through porous medium over an extending sheet with PST and PHF conditions." *International Journal of Applied and Computational Mathematics* 7, no. 6 (2021): 235. https://doi.org/10.1007/s40819-021-01137-9
[5] Waqas, Hassan, Sami Ullah Khan, S. A. Shehzad, M. Imran, and Iskander Tlili. "Activation energy and bioconvection aspects in generalized second-grade nanofluid over a Riga plate: a theoretical model." *Applied Nanoscience* 10 (2020): 4445-4458. https://doi.org/10.1007/s13204-020-01332-y
[6] Soomro, Feroz Ahmed, Muhammad Usman, Rizwan Ul Haq, and Wei Wang. "Melting heat transfer analysis of Sisko fluid over a moving surface with nonlinear thermal radiation via collocation method." *International Journal of Heat and Mass Transfer* 126 (2018): 1034-1042. https://doi.org/10.1016/j.ijheatmasstransfer.2018.05.099
[7] Tlili, Iskander, Sania Naseer, Muhammad Ramzan, Seifedine Kadry, and Yunyoung Nam. "Effects of chemical species and nonlinear thermal radiation with 3D Maxwell nanofluid flow with double stratification—an analytical solution." *Entropy* 22, no. 4 (2020): 453. https://doi.org/10.3390/e22040453
[8] Yahya, Asmat Ullah, Imran Siddique, Fahd Jarad, Nadeem Salamat, Sohaib Abdal, Y. S. Hamed, Khadijah M. Abualnaja, and Sajjad Hussain. "On the enhancement of thermal transport of Kerosene oil mixed TiO2 and SiO2 across Riga wedge." *Case Studies in Thermal Engineering* 34 (2022): 102025. https://doi.org/10.1016/j.csite.2022.102025

[9] Hanif, Hanifa, and Sharidan Shafie. "Interaction of multi-walled carbon nanotubes in mineral oil based Maxwell nanofluid." *Scientific Reports* 12, no. 1 (2022): 4712. https://doi.org/10.1038/s41598-022-07958-y
[10] Hanif, Hanifa, and Sharidan Shafie. "Impact of Al2O3 in electrically conducting mineral oil-based maxwell nanofluid: application to the petroleum industry." *Fractal and Fractional* 6, no. 4 (2022): 180. https://doi.org/10.3390/fractalfract6040180
[11] Siddique, Imran, Usama Habib, Rifaqat Ali, Sohaib Abdal, and Nadeem Salamat. "Bioconvection attribution for effective thermal transportation of upper convicted Maxwell nanofluid flow due to an extending cylindrical surface." *International Communications in Heat and Mass Transfer* 137 (2022): 106239. https://doi.org/10.1016/j.icheatmasstransfer.2022.106239
[12] Wang, Wen, Mohammed MM Jaradat, Imran Siddique, Abd Allah A. Mousa, Sohaib Abdal, Zead Mustafa, and Hafiz Muhammad Ali. "On thermal distribution for Darcy–Forchheimer flow of Maxwell Sutterby nanofluids over a radiated extending surface." *Nanomaterials* 12, no. 11 (2022): 1834. https://doi.org/10.3390/nano12111834
[13] Bilal, M., Hadia Tariq, Y. Urva, Imran Siddique, S. Shah, T. Sajid, and M. Nadeem. "A novel nonlinear diffusion model of magneto-micropolar fluid comprising Joule heating and velocity slip effects." *Waves in random and complex media* (2022): 1-17. https://doi.org/10.1080/17455030.2022.2079761
[14] Darcy, Henry. *Les fontaines publiques de Dijon*. 1856.
[15] Ph, Forchheimer. "Wasserbewegung durch boden." *Zeitschrift des Vereines Deutscher Ingenieure* 45, no. 50 (1901): 1781-1788.
[16] Muskat, Morris. "The flow of homogeneous fluids through porous media." *Soil Science* 46, no. 2 (1938): 169. https://doi.org/10.1097/00010694-193808000-00008
[17] Pal, Dulal, and Hiranmoy Mondal. "Hydromagnetic convective diffusion of species in Darcy–Forchheimer porous medium with non-uniform heat source/sink and variable viscosity." *International Communications in Heat and Mass Transfer* 39, no. 7 (2012): 913-917. https://doi.org/10.1016/j.icheatmasstransfer.2012.05.012
[18] Ganesh, N. Vishnu, AK Abdul Hakeem, and B. Ganga. "Darcy–Forchheimer flow of hydromagnetic nanofluid over a stretching/shrinking sheet in a thermally stratified porous medium with second order slip, viscous and Ohmic dissipations effects." *Ain Shams Engineering Journal* 9, no. 4 (2018): 939-951. https://doi.org/10.1016/j.asej.2016.04.019
[19] Alshomrani, Ali Saleh, and Malik Zaka Ullah. "Effects of homogeneous–heterogeneous reactions and convective condition in Darcy–Forchheimer flow of carbon nanotubes." *Journal of Heat Transfer* 141, no. 1 (2019): 012405. https://doi.org/10.1115/1.4041553
[20] Saif, Rai Sajjad, T. Hayat, R. Ellahi, Taseer Muhammad, and A. Alsaedi. "Darcy–Forchheimer flow of nanofluid due to a curved stretching surface." *International Journal of Numerical Methods for Heat & Fluid Flow* 29, no. 1 (2018): 2-20. https://doi.org/10.1108/HFF-08-2017-0301
[21] Seth, G. S., R. Kumar, and A. Bhattacharyya. "Entropy generation of dissipative flow of carbon nanotubes in rotating frame with Darcy-Forchheimer porous medium: A numerical study." *Journal of Molecular Liquids* 268 (2018): 637-646. https://doi.org/10.1016/j.molliq.2018.07.071
[22] Hanif, Hanifa, Sharidan Shafie, Noraihan Afiqah Rawi, and Abdul Rahman Mohd Kasim. "Entropy analysis of magnetized ferrofluid over a vertical flat surface with variable heating." *Alexandria Engineering Journal* 65 (2023): 897-908. https://doi.org/10.1016/j.aej.2022.09.052
[23] Chamkha, Ali J. "Non-Darcy hydromagnetic free convection from a cone and a wedge in porous media." *International communications in heat and mass transfer* 23, no. 6 (1996): 875-887. https://doi.org/10.1016/0735-1933(96)00070-X
[24] Hanif, Hanifa, and Sharidan Shafie. "Application of Cattaneo heat flux to Maxwell hybrid nanofluid model: a numerical approach." *The European Physical Journal Plus* 137, no. 8 (2022): 989. https://doi.org/10.1140/epjp/s13360-022-03209-1
[25] Jawad, Muhammad, Anwar Saeed, Poom Kumam, Zahir Shah, and Aurangzeb Khan. "Analysis of boundary layer MHD Darcy-Forchheimer radiative nanofluid flow with soret and dufour effects by means of marangoni convection." *Case Studies in Thermal Engineering* 23 (2021): 100792. https://doi.org/10.1016/j.csite.2020.100792
[26] Krishna, M. Veera, N. Ameer Ahamad, and Ali J. Chamkha. "Hall and ion slip effects on unsteady MHD free convective rotating flow through a saturated porous medium over an exponential accelerated plate." *Alexandria Engineering Journal* 59, no. 2 (2020): 565-577. https://doi.org/10.1016/j.aej.2020.01.043
[27] Hanif, Hanifa, Sharidan Shafie, Rozaini Roslan, and Anati Ali. "Collision of hybrid nanomaterials in an upper-convected Maxwell nanofluid: A theoretical approach." *Journal of King Saud University-Science* 35, no. 1 (2023): 102389. https://doi.org/10.1016/j.jksus.2022.102389
[28] Krishna, M. Veera, N. Ameer Ahamad, and Ali J. Chamkha. "Hall and ion slip impacts on unsteady MHD convective rotating flow of heat generating/absorbing second grade fluid." *Alexandria Engineering Journal* 60, no. 1 (2021): 845-858. https://doi.org/10.1016/j.aej.2020.10.013

[29] Tayebi, Tahar, A. Sattar Dogonchi, Nader Karimi, Hu Ge-JiLe, Ali J. Chamkha, and Yasser Elmasry. "Thermo-economic and entropy generation analyses of magnetic natural convective flow in a nanofluid-filled annular enclosure fitted with fins." *Sustainable Energy Technologies and Assessments* 46 (2021): 101274. https://doi.org/10.1016/j.seta.2021.101274

[30] Hanif, Hanifa, Ilyas Khan, and Sharidan Shafie. "A novel study on hybrid model of radiative Cu–Fe 3 O 4/water nanofluid over a cone with PHF/PWT: Hybrid model of radiative Cu–Fe 3 O 4/water nanofluid." *The European Physical Journal Special Topics* 230, no. 5 (2021): 1257-1271. https://doi.org/10.1140/epjs/s11734-021-00042-y

[31] Tayebi, Tahar. "Analysis of the local non-equilibria on the heat transfer and entropy generation during thermal natural convection in a non-Darcy porous medium." *International Communications in Heat and Mass Transfer* 135 (2022): 106133. https://doi.org/10.1016/j.icheatmasstransfer.2022.106133

[32] Tayebi, Tahar, and Ali J. Chamkha. "Analysis of the effects of local thermal non-equilibrium (LTNE) on thermo-natural convection in an elliptical annular space separated by a nanofluid-saturated porous sleeve." *International Communications in Heat and Mass Transfer* 129 (2021): 105725. https://doi.org/10.1016/j.icheatmasstransfer.2021.105725

[33] Tayebi, Tahar, Ali J. Chamkha, Hakan F. Öztop, and Lynda Bouzeroura. "Local thermal non-equilibrium (LTNE) effects on thermal-free convection in a nanofluid-saturated horizontal elliptical non-Darcian porous annulus." *Mathematics and Computers in Simulation* 194 (2022): 124-140. https://doi.org/10.1016/j.matcom.2021.11.011

[34] Hussain, S., T. Tayebi, T. Armaghani, A. M. Rashad, and H. A. Nabwey. "Conjugate natural convection of non-Newtonian hybrid nanofluid in wavy-shaped enclosure." *Applied Mathematics and Mechanics* 43, no. 3 (2022): 447-466. https://doi.org/10.1007/s10483-022-2837-6

[35] Choi, S. US, and Jeffrey A. Eastman. *Enhancing thermal conductivity of fluids with nanoparticles*. No. ANL/MSD/CP-84938; CONF-951135-29. Argonne National Lab.(ANL), Argonne, IL (United States), 1995.

[36] Shafiq, Anum, S. A. Lone, Tabassum Naz Sindhu, Q. M. Al-Mdallal, and G. Rasool. "Statistical modeling for bioconvective tangent hyperbolic nanofluid towards stretching surface with zero mass flux condition." *Scientific Reports* 11, no. 1 (2021): 13869. https://doi.org/10.1038/s41598-021-93329-y

[37] Sadiq, Kashif, Fahd Jarad, Imran Siddique, and Bagh Ali. "Soret and Radiation Effects on Mixture of Ethylene Glycol-Water (50%-50%) Based Maxwell Nanofluid Flow in an Upright Channel." *Complexity* 2021, no. 1 (2021): 5927070. https://doi.org/10.1155/2021/5927070

[38] Siddique, Imran, Rana Muhammad Zulqarnain, Muhammad Nadeem, and Fahd Jarad. "Numerical simulation of MHD Couette flow of a fuzzy nanofluid through an inclined channel with thermal radiation effect." *Computational Intelligence and Neuroscience* 2021, no. 1 (2021): 6608684. https://doi.org/10.1155/2021/6608684

[39] Nadeem, Muhammad, Imran Siddique, Muhammad Bilal, and Rifaqat Ali. "Significance of heat transfer for second-grade fuzzy hybrid nanofluid flow past over a stretching/shrinking riga wedge." (2022). https://doi.org/10.21203/rs.3.rs-1629830/v1

[40] Siddique, Imran, Kashif Sadiq, Ilyas Khan, and Kottakkaran Sooppy Nisar. "Nanomaterials in convection flow of nanofluid in upright channel with gradients." *Journal of Materials Research and Technology* 11 (2021): 1411-1423. https://doi.org/10.1016/j.jmrt.2021.01.002

[41] Siddique, Imran, Muhammad Nadeem, Ilyas Khan, Raja Noshad Jamil, Mohamed A. Shamseldin, and Ali Akgül. "Analysis of fuzzified boundary value problems for MHD Couette and Poiseuille flow." *Scientific Reports* 12, no. 1 (2022): 8368. https://doi.org/10.1038/s41598-022-12110-x

[42] Roy, Nepal Chandra, and Ioan Pop. "Exact solutions of Stokes' second problem for hybrid nanofluid flow with a heat source." *Physics of Fluids* 33, no. 6 (2021). https://doi.org/10.1063/5.0054576

[43] Shehzad, S. A., M. Sheikholeslami, T. Ambreen, Ahmad Shafee, Houman Babazadeh, and M. Ahmad. "Heat transfer management of hybrid nanofluid including radiation and magnetic source terms within a porous domain." *Applied Nanoscience* 10 (2020): 5351-5359. https://doi.org/10.1007/s13204-020-01432-9

[44] Acharya, Nilankush, and Fazle Mabood. "On the hydrothermal features of radiative Fe3O4–graphene hybrid nanofluid flow over a slippery bended surface with heat source/sink." *Journal of Thermal Analysis and Calorimetry* 143, no. 2 (2021): 1273-1289. https://doi.org/10.1007/s10973-020-09850-1

[45] Chamkha, Ali J., Rizk Yassen, Muneer A. Ismael, A. M. Rashad, T. Salah, and Hossam A. Nabwey. "MHD free convection of localized heat source/sink in hybrid nanofluid-filled square cavity." *Journal of Nanofluids* 9, no. 1 (2020): 1-12. https://doi.org/10.1166/jon.2020.1726

[46] Ghachem, Kaouther, Walid Aich, and Lioua Kolsi. "Computational analysis of hybrid nanofluid enhanced heat transfer in cross flow micro heat exchanger with rectangular wavy channels." *Case Studies in Thermal Engineering* 24 (2021): 100822. https://doi.org/10.1016/j.csite.2020.100822

[47] Yahya, Asmat Ullah, Nadeem Salamat, Wen-Hua Huang, Imran Siddique, Sohaib Abdal, and Sajjad Hussain. "Thermal charactristics for the flow of Williamson hybrid nanofluid (MoS2+ ZnO) based with engine oil over a

streched sheet." *Case Studies in Thermal Engineering* 26 (2021): 101196. https://doi.org/10.1016/j.csite.2021.101196
[48] Nadeem, Muhammad, Imran Siddique, Jan Awrejcewicz, and Muhammad Bilal. "Numerical analysis of a second-grade fuzzy hybrid nanofluid flow and heat transfer over a permeable stretching/shrinking sheet." *Scientific Reports* 12, no. 1 (2022): 1631. https://doi.org/10.1038/s41598-022-05393-7
[49] Nadeem, Muhammad, Ahmed Elmoasry, Imran Siddique, Fahd Jarad, Rana Muhammad Zulqarnain, Jawdat Alebraheem, and Naseer S. Elazab. "Study of triangular fuzzy hybrid nanofluids on the natural convection flow and heat transfer between two vertical plates." *Computational Intelligence and Neuroscience* 2021, no. 1 (2021): 3678335. https://doi.org/10.1155/2021/3678335
[50] Adun, Humphrey, Doga Kavaz, and Mustafa Dagbasi. "Review of ternary hybrid nanofluid: Synthesis, stability, thermophysical properties, heat transfer applications, and environmental effects." *Journal of Cleaner Production* 328 (2021): 129525. https://doi.org/10.1016/j.jclepro.2021.129525
[51] Sundar, L. Syam, Kotturu VV Chandra Mouli, Zafar Said, and Antonio CM Sousa. "Heat transfer and second law analysis of ethylene glycol-based ternary hybrid nanofluid under laminar flow." *Journal of Thermal Science and Engineering Applications* 13, no. 5 (2021): 051021. https://doi.org/10.1115/1.4050228
[52] Ahmed, Waqar, Salim Newaz Kazi, Zaira Zaman Chowdhury, Mohd Rafie Bin Johan, Shahid Mehmood, Manzoore Elahi M. Soudagar, M. A. Mujtaba, M. Gul, and Muhammad Shakeel Ahmad. "Heat transfer growth of sonochemically synthesized novel mixed metal oxide ZnO+ Al2O3+ TiO2/DW based ternary hybrid nanofluids in a square flow conduit." *Renewable and sustainable energy reviews* 145 (2021): 111025. https://doi.org/10.1016/j.rser.2021.111025
[53] Arif, Muhammad, Poom Kumam, Wiyada Kumam, and Zaydan Mostafa. "Heat transfer analysis of radiator using different shaped nanoparticles water-based ternary hybrid nanofluid with applications: A fractional model." *Case Studies in Thermal Engineering* 31 (2022): 101837. https://doi.org/10.1016/j.csite.2022.101837
[54] Gul, Taza, and Anwar Saeed. "Nonlinear mixed convection couple stress tri-hybrid nanofluids flow in a Darcy–Forchheimer porous medium over a nonlinear stretching surface." *Waves in Random and Complex Media* (2022): 1-18. https://doi.org/10.1080/17455030.2022.2077471
[55] Nadeem, Muhammad, Imran Siddique, Fahd Jarad, and Raja Noshad Jamil. "Numerical Study of MHD Third-Grade Fluid Flow through an Inclined Channel with Ohmic Heating under Fuzzy Environment." *Mathematical Problems in Engineering* 2021, no. 1 (2021): 9137479. https://doi.org/10.1155/2021/9137479
[56] Jan, Ahmed, Muhammad Mushtaq, Umer Farooq, and Muzamil Hussain. "Nonsimilar analysis of magnetized Sisko nanofluid flow subjected to heat generation/absorption and viscous dissipation." *Journal of Magnetism and Magnetic Materials* 564 (2022): 170153. https://doi.org/10.1016/j.jmmm.2022.170153.
[57] Jan, Ahmed, Muhammad Mushtaq, and Muzamil Hussain. "Heat transfer enhancement of forced convection magnetized cross model ternary hybrid nanofluid flow over a stretching cylinder: non-similar analysis." *International Journal of Heat and Fluid Flow* 106 (2024): 109302. https://doi.org/10.1016/j.ijheatfluidflow.2024.109302.
[58] Farooq, Umer, Amara Bibi, Javeria Nawaz Abbasi, Ahmed Jan, and Muzamil Hussain. "Nonsimilar mixed convection analysis of ternary hybrid nanofluid flow near stagnation point over vertical Riga plate." *Multidiscipline Modeling in Materials and Structures* 20, no. 2 (2024): 261-278. https://doi.org/10.1108/MMMS-09-2023-0301
[59] Cui, Jifeng, Shahzad Munir, Syeda Faiza Raies, Umer Farooq, and Raheela Razzaq. "Non-similar aspects of heat generation in bioconvection from flat surface subjected to chemically reactive stagnation point flow of Oldroyd-B fluid." *Alexandria Engineering Journal* 61, no. 7 (2022): 5397-5411. https://doi.org/10.1016/j.aej.2021.10.056.
[60] Farooq, Javaria, Jae Dong Chung, Muhammad Mushtaq, Dianchen Lu, Muhammad Ramazan, and Umer Farooq. "Influence of slip velocity on the flow of viscous fluid through a porous medium in a permeable tube with a variable bulk flow rate." *Results in Physics* 11 (2018): 861-868. https://doi.org/10.1016/j.rinp.2018.10.049.
[61] Kumar, A., R. Tripathi, R. Singh, and V. K. Chaurasiya. "Simultaneous effects of nonlinear thermal radiation and Joule heating on the flow of Williamson nanofluid with entropy generation." *Physica A: Statistical Mechanics and its Applications* 551 (2020): 123972. https://doi.org/10.1016/j.physa.2019.123972.
[62] Kumar, A., and Rajendra K. Ray. "Shape effect of nanoparticles and entropy generation analysis for magnetohydrodynamic flow of A l 2 O 3-C u/H 2 O hybrid nanomaterial under the influence of Hall current." *Indian Journal of Physics* 96, no. 13 (2022): 3817-3830. https://doi.org/10.1007/s12648-022-02300-8
[63] Sethy, Priyabrata, Amit Kumar, Atul Kumar Ray, Abha Kumari, and Lalrinpuia Tlau. "Synergistic impacts of radiative flow of Maxwell fluid past a rotating disk with reactive conditions: An Arrhenius model analysis." *Chinese Journal of Physics* 89 (2024): 761-792. https://doi.org/10.1016/j.cjph.2024.03.018.
[64] Tripathi, R., V. K. Chaurasiya, A. Kumar, and R. Singh. "Minimization of entropy production in the transient thermocapillary flow of A l 2 O 3-C u hybrid nanoliquid film over a disk." *Indian Journal of Physics* 96, no. 5 (2022): 1465-1479. https://doi.org/10.1007/s12648-021-02100-6

[65] Kumar, Amit, Abhipsa P. Dash, Atul Kumar Ray, Priyabrata Sethy, and Idamakanti Kasireddy. "Unsteady mixed convective flow of hybrid nanofluid past a rotating sphere with heat generation/absorption: an impact of shape factor." *International Journal of Numerical Methods for Heat & Fluid Flow* 33, no. 11 (2023): 3691-3715. https://doi.org/10.1108/HFF-03-2023-0129